**Atmospheric
Chemistry
and Physics
Discussions**

Linear ozone
photochemistry
parametrizations

A. J. Geer et al.

Evaluation of linear ozone photochemistry parametrizations in a stratosphere-troposphere data assimilation system

A. J. Geer[1,2], W. A. Lahoz[1], D. R. Jackson[3], D. Cariolle[4], and J. P. McCormack[5]

[1]Data Assimilation Research Centre (DARC), University of Reading, Reading, UK
[2]Now at European Centre for Medium-Range Weather Forecasts (ECMWF), Reading, UK
[3]Met Office, Exeter, UK
[4]Centre Européen de Recherche et Formation Avancée en Calcul Scientifique (CERFACS),
Toulouse, France and Météo-France, Toulouse, France
[5]E. O. Hulburt Center for Space Research, Naval Research Laboratory (NRL), Washington
D.C., USA

Correspondence to: A. J. Geer (alan.geer@ecmwf.int)

Title Page	
Abstract	Introduction
Conclusions	References
Tables	Figures

◄◄	►►
◄	►
Back	Close

Full Screen / Esc

Printer-friendly Version

Interactive Discussion

EGU

Abstract

This paper evaluates the performance of various linear ozone photochemistry parametrizations using the stratosphere-troposphere data assimilation system of the Met Office. A set of experiments were run for the period 23 September 2003 to 5 November 2003 using the Cariolle (v1.0 and v2.1), LINOZ and Chem2D-OPP (v0.1 and v2.1) parametrizations. All operational meteorological observations were assimilated, together with ozone retrievals from the Michelson Interferometer for Passive Atmospheric Sounding (MIPAS). Experiments were validated against independent data from the Halogen Occultation Experiment (HALOE) and ozonesondes.

It is shown that the LINOZ scheme is unsuitable for use above 10 hPa, but below this level it works as well as the other schemes. The Cariolle v1.0 scheme shows excessive sensitivity in the term related to overlying column ozone, and this results in erroneous ozone production in the ozone hole. The other three schemes (Cariolle v2.1 and Chem2D-OPP v0.1 and v2.1) all perform well through most of the atmosphere. Exceptions were the troposphere, where modelling and observing ozone remains a substantial challenge, and the upper stratosphere and mesosphere, where the main problems come from biases in the schemes' climatology coefficients. Cariolle v2.1 analyses showed biases of up to 20% against HALOE at levels above 1 hPa. These biases could be partially corrected by substituting the Fortuin and Kelder (1998) ozone climatology into the scheme. Chem2D-OPP v2.1 analyses showed biases up to 20% and unrealistic ozone patterns in the southern hemisphere upper stratosphere, likely due to discrepancies between analysed temperatures and the temperature climatology supplied with the scheme. Future developments should include a better treatment of the troposphere, and a parametrization of the diurnal cycle of ozone above 0.5 hPa.

EGU

1 Introduction

Atmospheric ozone is of interest not just because of the problem of ozone depletion (e.g., WMO, 2003) but also for its basic role in controlling the temperature structure of the atmosphere through the absorption of solar and long-wave radiation. The distribution of atmospheric ozone results from the interaction of transport, chemistry, and radiation processes. A full description of the photochemistry of ozone would be extremely complicated, involving hundreds of chemical species and reactions, many of which are interlinked. A detailed approximation to this can be embodied in a chemistry-transport model (CTM) (e.g. Chipperfield, 1999; Rozanov et al., 1999; Errera and Fonteyn, 2001; Josse et al., 2004), which is driven by off-line meteorological analyses. However, in applications such as climate modelling and numerical weather prediction (NWP) or data assimilation (DA), it is often desirable to use a faster, simpler representation of ozone photochemistry.

Cariolle and Déqué (1986) developed a parametrization of ozone photochemistry based on a linearisation of the ozone tendency around an equilibrium state, using parameters derived from a CTM with more detailed chemistry. The parametrization depends only on temperature and ozone amount; hence no other chemically active species need be modelled. As well as saving computer resources, this prevents a mis-specified or poorly-known chemical species from causing a bias in the modelled ozone amount. Along with the original scheme of Cariolle and Déqué (1986, v1.0), a v2.1 has recently become available, and coefficients have been independently developed by McLinden et al. (2000, the LINOZ scheme) and McCormack et al. (2004, Chem2D-OPP). Table 1 summarises these developments. Linearised ozone photochemistry schemes are routinely used in data assimilation (e.g., Eskes et al., 2003; Dethof and Hólm, 2004; Geer et al., 2006a,b) and in multi-year climate simulations (e.g., Hadjinicolaou et al., 1997). Recently, Taylor and Bourqui (2005) developed a fast ozone photochemistry scheme of intermediate complexity, but this paper concentrates on the much-used linear approach.

A number of studies have indicated problems in the earlier generation of linear photochemistry schemes and the ozone distributions that they produce. LINOZ is unsuitable for use in the upper stratosphere (McCormack et al., 2004; Geer et al., 2006a). Version 1.0 of Cariolle and Déqué (1986) has a strong sensitivity to the overlying ozone amount (Geer et al., 2006b). Even small ozone differences can be important in general circulation models (GCMs): ~10% variations in ozone amounts can result in changes in modelled temperatures of several Kelvin (Cariolle and Morcrette, 2006). Now that updated photochemistry schemes are available, it is useful to evaluate and understand their differences. The data assimilation (DA) framework presents an opportunity to do this. Computational limitations mean that only a short period can be examined in the DA system used here, and much longer-term evaluation inside CTMs is clearly necessary. However, the DA framework presents one major advantage: free-running models can evolve to a state that may be different from the real atmosphere; the regular insertion of observational data in a DA system acts to prevent this.

We examine the performance of a number of different ozone photochemistry schemes in the stratosphere-troposphere DA system of the Met Office. 3-D-Variational data assimilation (3D-Var) is used to assimilate all operational dynamical observations, plus ozone retrievals from the Michelson Interferometer for Passive Atmospheric Sounding (MIPAS) on the Envisat satellite. The analyses are validated against independent ozone data from sondes and the Halogen Occultation Experiment (HALOE).

2 Ozone chemistry schemes

2.1 Photochemistry parametrization

The rate of change of ozone due to photochemistry can be written (Cariolle and Déqué, 1986) as a first order Taylor expansion about the ozone production rate (P) minus loss

rate (L), at an equilibrium state:

$$C = (P - L)_0 + \left.\frac{\partial(P - L)}{\partial \chi}\right|_0 (\chi - \chi_0) +$$
$$\left.\frac{\partial(P - L)}{\partial T}\right|_0 (T - T_0) + \left.\frac{\partial(P - L)}{\partial \Phi}\right|_0 (\Phi - \Phi_0). \tag{1}$$

This parametrization has three variables: the local ozone mixing ratio, χ (in this paper as mass mixing ratio in units of $kg\,kg^{-1}$); the temperature, T, in K, and the column of ozone overlying the level under consideration, Φ, in $kg\,m^{-2}$, where:

$$\Phi = 1/g \int_{TOA}^{l} \chi \, dp, \tag{2}$$

and the integral runs over all pressure levels from the top of the atmosphere (TOA) down to level l. All other items in Eq. (1) are coefficients valid at the equilibrium state (denoted with the subscript 0) which are either climatological values or have been pre-calculated with a detailed photochemical model. They are given as functions of latitude, model level and month; hence there is no diurnal or longitudinal variation. They include the climatological values of ozone, χ_0, temperature, T_0, and the overlying column of ozone, Φ_0, which is calculated from vertical profiles of χ_0 using Eq. (2).

The first term in the expansion is the equilibrium ozone production rate minus loss rate, $(P-L)_0$. The second term accounts for variations in the local ozone amount, the third for temperature and the last term for the influence of non-local ozone on the amount of solar radiation reaching the level in question, and here we will call it the radiation term. Though the photochemistry parametrization causes no diurnal variation, it should be remembered that there is in reality a diurnal cycle of ozone which starts to become significant at levels above 0.5 hPa, in the mesosphere.

Title Page

Abstract | Introduction

Conclusions | References

Tables | Figures

◄◄ | ►►

◄ | ►

Back | Close

Full Screen / Esc

Printer-friendly Version

Interactive Discussion

EGU

In the DARC implementation, the radiation term has been modified by substituting the following into Eq. (1):

$$\Phi - \Phi_0 = 1/g \int_{TOA}^{l} (\chi - \chi_0)\,dp. \tag{3}$$

We have used Eqs. (2) and (3) to eliminate the overlying column climatology, Φ_0, from the parametrization. Though it may seem trivial, this modification means that Φ and Φ_0 are calculated implicitly using consistent methods. If they were not calculated consistently, the radiation term could produce a forcing even if $\chi = \chi_0$ throughout the overlying column. With this modification, Φ_0 no longer needs to be recalculated from χ_0 each time the model's vertical resolution changes. Neglecting to do this, and instead interpolating Φ_0 to a new set of vertical levels, caused a $\sim$40% model bias in the lower mesosphere in the DARC/Met Office assimilation experiments examined in Geer et al. (2006a).

We can explore the effect of the parametrization by considering the ozone budget in a hypothetical model, which will include the rates of change of ozone due to modelled ozone transport, A, and chemistry, C (from Eq. 1):

$$\frac{\partial \chi}{\partial t} = A + C. \tag{4}$$

Ignoring for simplicity the temperature and radiation terms in C, and assuming transport, A, is constant, we can define a steady state mixing ratio:

$$\chi_{ss} \equiv \chi_0 + [(P - L)_0 + A]\tau, \tag{5}$$

and the photochemical relaxation time,

$$\tau \equiv -1 \Big/ \left(\frac{\partial (P - L)}{\partial \chi} \bigg|_0 \right). \tag{6}$$

Linear ozone photochemistry parametrizations

A. J. Geer et al.

Title Page

Abstract	Introduction
Conclusions	References
Tables	Figures

◄◄ ►►

◄ ►

Back Close

Full Screen / Esc

Printer-friendly Version

Interactive Discussion

EGU

This allows us to solve Eq. (4) analytically, showing that with steady-state transport (and ignoring temperature and radiation terms), the linearised ozone photochemistry scheme will cause modelled ozone to follow an exponential relaxation to steady state, χ_{ss}, with a time constant τ:

$$\chi^{t+\Delta t} = \chi^t + (\chi_{ss} - \chi^t)(1 - e^{-\Delta t/\tau}), \tag{7}$$

Ozone amounts χ^t and $\chi^{t+\Delta t}$ apply at times t and $t+\Delta t$ respectively. Note that Eqs. (5) and (7) differ from the treatment given in McLinden et al. (2000), because here, the effects of transport are included.

Figure 1 shows the October value of τ, the photochemical relaxation time, from the Cariolle v1.0 parametrization. In the upper stratosphere, τ is less than a day and the ozone fields are essentially in photochemical equilibrium. If perturbed away from this equilibrium, ozone fields will quickly relax back to it. Lower in the stratosphere, photochemical relaxation times are much longer, with $\tau > 100$ days at 100 hPa. Here, modelled transport has an important control over the ozone field.

Equation (5) encapsulates the climatological balance between photochemistry and transport. If the steady state ozone amount generated by the photochemistry scheme is to be equal to climatological ozone, χ_0, Eq. (5) requires either that modelled ozone transport must balance the net equilibrium production or loss due to photochemistry, i.e. $(P-L)_0 + A = 0$, or that $\tau \to 0$. Hence in this example, ozone will always be close to climatology in regions where the photochemical relaxation time is short. In the mid and lower stratosphere and troposphere, relaxation times are relatively long (Fig. 1). Here, the steady-state example reflects real-life behaviour: In the lower stratosphere, for example, net photochemical production in the tropics is approximately balanced by the upward and poleward transport of ozone in the Brewer-Dobson circulation (e.g., Plumb et al., 2002); there is a net photochemical loss at higher latitudes.

2.1.1 Practical considerations

In the case of the radiation term, we have already seen that an incorrectly implemented linear photochemistry scheme can generate a spurious photochemical tendency (Eq. 3 and following discussion). The same principle applies to the other terms in the photochemistry scheme.

Equations (5) and (7) show that if modelled ozone transport A does not balance the equilibrium photochemical tendency $(P-L)_0$, modelled ozone will relax toward a steady state (χ_{ss}) that is different from climatology (χ_0). If modelled ozone transport were different from climatology because of natural variability, of course this would be a desirable result. However, particularly in data assimilation systems, stratospheric constituent transport can be erroneously fast (e.g., Schoeberl et al., 2003). Especially where the photochemical relaxation time τ is relatively long, i.e. in the mid and lower stratosphere, the linear photochemistry scheme cannot correct for such transport errors. Geer et al. (2006b) showed how an excessively fast modelled Brewer-Dobson circulation caused biases in the DARC/Met Office ozone analyses.

In the troposphere, it is important to account for ozone transport by convection and boundary layer processes. In the CTM used to generate the photochemistry coefficients, these processes may be parametrized through the use of vertical diffusion. In the GCM in which the ozone photochemistry parametrization is to be used, convection and boundary layer processes will be more explicitly resolved, though still heavily parametrized. If modelled transport A, differs between the CTM and the GCM, the equilibrium photochemical tendency $(P-L)_0$ will be consistent with the CTM, but not the GCM. Again, this could cause ozone amounts to be biased in the GCM.

In data assimilation applications it is necessary that model and observations should be unbiased with respect to one another. If the model were relaxing to steady state (Eq. 7), would this state be unbiased with respect to the climatology of assimilated ozone observations? It is usual to find small biases between different instruments and different climatologies. Hence, it is typical in data assimilation applications (e.g., Eskes

Linear ozone photochemistry parametrizations

A. J. Geer et al.

EGU

et al., 2003) to use a new ozone climatology (χ_0) in place of the one supplied with the photochemistry scheme. It is hoped that the new climatology will be less biased with respect to observations. Often, as in this study, the Fortuin and Kelder (1998) climatology is chosen. Later we suggest that it may actually be necessary to use a
5 climatology based on the observations being assimilated.

    Similar considerations apply to the temperature climatology. If climatological mean temperatures in the model were different from those used in the photochemistry scheme, T_0, the temperature term (see Eq. 1) would on average produce a net forcing in ozone. This is undesirable as it would add an extra forcing term in the brack-
10 ets in Eq. (5), and even if climatological transport and photochemistry were balanced ($(P-L)_0+A=0$), the model would relax to a steady state that would be different from climatology. Figure 2 compares the monthly mean analysed temperature for October 2003 to T_0 from three of the chemistry schemes used here. The climatologies and the DARC/Met Office analyses show differences of up to 20 K. Between 6 and 30 hPa
15 at 80°S there is a warm bulge in Met Office temperatures, compared to climatology, and this is likely due to the strong minor warming that took place during October 2003 (Lahoz et al., 2006, see also Fig. 10). Randel et al. (2004) found that the CIRA86 climatology, as used in Chem2D-OPP v2.1, has a 5–10 K warm bias through much of the stratosphere. This is consistent with the positive bias seen in CIRA86 temperatures in
20 Fig. 2, compared to the other climatologies, particularly around the stratopause.

    The results later in this paper illustrate the problems that can be caused by discrepancies between the parametrization's ozone (χ_0) and temperature (T_0) climatologies and the modelled or observed equivalents. However, a more careful choice of χ_0 and T_0 will likely improve analysed ozone distributions. In contrast, there is no easy solution
25 to the problem of erroneous or mis-matched ozone transport; this particularly affects lower stratosphere ozone amounts.

2.2 Heterogeneous chemistry

Heterogeneous ozone chemistry must be modelled in order to describe ozone deple-tion in the spring polar vortex (e.g. WMO, 2003). Though the Cariolle v2.1 chemistry scheme does include a simple parametrization of ozone depletion, this paper does not attempt to test it. Instead, in all experiments, heterogeneous chemistry is parametrized by a cold tracer scheme (Eskes et al., 2003). The focus here is on photochemistry, and the heterogeneous chemistry is kept fixed.

In other models, the cold tracer scheme has enabled a good simulation of ozone depletion even without data assimilation (Eskes et al., 2005). The Assimilation of Envisat Data (ASSET) intercomparison (Geer et al., 2006a) examined analyses based on models with many different treatments of heterogeneous chemistry, includ-ing DARC/MetOffice ozone analyses made with a system similar to that used here. The DARC/MetOffice analyses performed adequately well in the ozone-hole, though amounts were not depleted to the near-zero values observed by sondes. This was due not to deficiencies in the cold tracer scheme, but instead to erroneous ozone produc-tion in the radiation term of the Cariolle v1.0 photochemistry scheme. Later we show that ozone depletion is well represented in the analyses when the cold tracer scheme is used with any of the other photochemistry parametrizations.

2.3 Cariolle and Déqué (1986) v1.0 and v2.1

The Cariolle v1.0 scheme is described by Cariolle and Déqué (1986) and was cal-culated using a 2-D photochemical model with an upper boundary at 1 hPa, and by extrapolation or from 1-D model results above that level.

The subsequent v2.1 scheme is described by Cariolle and Teyssédre (2006)[1]. It has been derived using the same 2-D photochemical model as for v1.0 except that

---

[1]Cariolle, D. and Teyssédre, H.: A revised linear ozone photochemistry parametrization for use in transport and general circulation model. I. Multi-year simulations, in preparation, 2006.

EGU

the gas-phase chemical rates have been upgraded using the JPL (2003) recommendations, and that the residual meridional circulation used for minor tracer transport is derived from a 10 year simulation of the Arpège-Climat general circulation model. Equally, the temperature distribution comes from the same GCM simulation. The vertical and horizontal resolutions of the 2-D model have also been increased to match the Arpège-Climat discretisation. The 2-D model has 45 vertical levels extending up to 0.1 hPa, 64 latitudes, and accounts for the photochemistry of 63 species, 29 of which are transported.

The partial derivatives appearing in Eq. (1) are obtained by perturbing the 2-D model fields by ±10% for the ozone mixing ratio (more precisely the odd oxygen family) and the ozone column, and by ±10 K for the temperature. For each perturbed case the non-transported short lived species are re-evaluated at steady state and the ozone production and loss rates are used in the partial derivatives calculations. This is done for every month and a set of 7 zonal mean coefficients are obtained.

Three configurations of the Cariolle parameters are tested: (a) using the supplied ozone climatology in the v2.1 scheme, (b) instead using Fortuin and Kelder (1998) climatology in the v2.1 scheme, and (c) using Fortuin and Kelder (1998) climatology in the v1.0 scheme.

Note that the Cariolle v2.1 heterogeneous ozone depletion term is not tested here; the cold tracer scheme (Eskes et al., 2003) was used in all experiments. Separately, it has been found that, combined with the assimilation of MIPAS data, the simple heterogeneous chemistry parametrization in the Cariolle v2.1 scheme works as well as more detailed heterogeneous chemistry schemes (Geer et al., 2006a).

2.4 LINOZ

The LINOZ scheme is described by McLinden et al. (2000). The coefficients in Eq. (1) were calculated for 12 months between 85° S and 85° N and and at 25 altitudes between 10 to 58 km using a photochemical box model (Prather and Jaffe, 1990; Prather, 1992). This model includes 109 kinetic reactions, 36 photolysis reactions and 43

Linear ozone photochemistry parametrizations

A. J. Geer et al.

species, and reaction coefficients and absorption cross-sections are adopted from De-More et al. (1997). For each monthly calculation, the box model is integrated for 30 days with the diurnal cycle fixed at mid-month. The ozone tendency and partial derivatives (see Eq. 1) are diurnally averaged.

5   Originally, the ozone and column ozone climatologies from McPeters (1993) and the temperature climatology from Nagatani and Rosenfield (1993) were used. Here instead we substitute the ozone climatology of Fortuin and Kelder (1998).

LINOZ coefficients are not available below 10 km. Geer et al. (2006a) found that in the troposphere, a relaxation to ozone climatology produced smaller biases compared

10   to ozonesonde than did the full linear chemistry parametrizations. Hence for LINOZ in these tests, below 10 km, a relaxation to Fortuin and Kelder (1998) climatology was implemented, using the photochemical relaxation times of Cariolle v1.0.

2.5   Chem2D-OPP v0.1 and v2.1

Chem2D-OPP is described by McCormack et al. (2004), for v0.1, and by McCormack

15   et al. (2006) for v2.1; see http://uap-www.nrl.navy.mil/dynamics/html/chem2dopp/ chem2d_opp.html for updates. Photochemistry coefficients are computed with the NRL-Chem2D middle atmosphere photochemical-transport model (Siskind et al., 2003). The Chem2D model domain extends from pole to pole and from the surface up to $p=2\times10^{-5}$ hPa ($\sim$122 km altitude), with 47 vertical levels. The middle atmospheric

20   radiative heating, photochemistry, and transport are fully coupled. Chem2D photochemistry accounts for 54 chemical species and uses updated JPL (2003) reaction rates. Diurnally averaged photolysis rates are computed by averaging hourly values, and diurnally averaged reaction rate coefficients are derived from pre-computed night-day ratios of relevant species. Solar irradiance for calculating both photolysis and UV

25   radiative heating is specified as a function of wavelength from 120–800 nm, including Lyman-α and both the Schumann-Runge continuum and Schumann-Runge bands for O_2 photolysis.

Chem2D-OPP v0.1 includes the first two terms from the right hand side of Eq. (1)

Linear ozone photochemistry parametrizations

A. J. Geer et al.

EGU

and does not account for temperature or radiation effects (McCormack et al., 2004). Diurnally averaged values of the Chem2D net ozone tendency $(P-L)_0$ are computed for the 15th day of each month. The partial derivative with respect to mixing ratio, $\frac{\partial(P-L)}{\partial\chi}|_0$ in Eq. (1), is calculated as the negative inverse of the ozone photochemical relaxation time τ. The latter is determined from the sum of individual loss rates involving reactions with NO_x, Cl_x, and HO_x. The results are tabulated as functions of latitude, pressure, and month and then interpolated onto a $10°$ latitude grid at standard pressure levels from 1000–0.001 hPa.

Chem2D-OPP v2.1 includes all four of the terms in Eq. (1). In the present study, the v2.1 $(P-L)_o$ and $\frac{\partial(P-L)}{\partial\chi}|_0$ coefficients are computed as in Chem2d-OPP v0.1. To evaluate the temperature and column ozone coefficients, $\frac{\partial(P-L)}{\partial T}|_0$ and $\frac{\partial(P-L)}{\partial\Phi}|_0$, respectively, the Chem2D model computes $(P-L)_0$ for a given altitude, latitude, and time of year, then immediately repeats the calculation using identical model constituent fields and a perturbation in either temperature or overlying ozone column amount. In the temperature case, perturbations (ΔT) between $\pm20\,\mathrm{K}$ are imposed and the entire chemical system is then solved with an iterative Newton-Raphson technique until the $(P-L)$ values converge to a new equilibrium state. Similarly, the coefficient $\frac{\partial(P-L)}{\partial\Phi}|_0$ is evaluated by introducing ozone column perturbations $\Delta\Phi$ between $\pm50\%$ to the Chem2D UV transmission functions used to compute the O_2 and O_3 photolysis rates. For a more detailed description of this method see McCormack et al. (2006).

The Chem2D model uses fixed heating rates at the surface as a model boundary condition and so the radiative heating is not coupled to model ozone in the lowermost model levels. For implementation in the DARC system, the v2.1 radiation term was turned off below 500 hPa as it was suspected it would not work well in the lower troposphere. Surface values of the v2.1 photochemical relaxation time were erroneously negative due to an error in the vertical interpolation scheme, and this would have caused a runaway growth in ozone amounts. To prevent this happening, τ was reset to $\sim+2$ days at the surface. This problem has been fixed in a more recent version of the

Linear ozone photochemistry parametrizations

A. J. Geer et al.

Title Page

Abstract | Introduction

Conclusions | References

Tables | Figures

◄◄ | ►►

◄ | ►

Back | Close

Full Screen / Esc

Printer-friendly Version

Interactive Discussion

EGU

Chem2D-OPP coefficients (v2.4), which also contains updated values for $\frac{\partial(P-L)}{\partial\chi}\big|_0$ that now include Br_x effects. We do not test version 2.4 here.

2.6 Offline comparison of photochemistry schemes

We can examine the relative strengths of the terms in the different schemes by testing their sensitivity to a representative perturbation in ozone or temperature (Fig. 3). For ozone, we used a perturbation based on the climatological ozone standard deviations of Fortuin and Kelder (1998), given as a function of month, pressure and latitude. For the overlying ozone column, we calculated the partial column integral of these standard deviations using Eq. (2). For temperature, we assumed a uniform perturbation of 5 K, though around the wintertime polar vortex, stratospheric temperatures can vary by much larger amounts.

For each month, latitude and pressure level, the change in the net photochemical ozone tendency caused by the perturbation was normalised by the climatological ozone amount, χ_0. For example, the sensitivity to changes in local ozone was calculated as:

$$\Delta C = \frac{\sigma_\chi}{\chi_0} \frac{\partial(P-L)}{\partial\chi}\bigg|_0, \tag{8}$$

where σ_χ is the climatological ozone standard deviation. We then converted ΔC to units of %day^{-1}. The net climatological ozone tendency, $(P-L)_0$, was normalised by the climatological ozone amount so that it could be examined in the same units. At each pressure level, and for each month, global means (equal weight by latitude) were calculated from the absolute value of ΔC. Figure 3 shows the resulting estimates of the sensitivity of the different terms for October. In general, the schemes have least influence on the ozone amount around the tropopause, and larger influence in the troposphere, upper stratosphere and mesosphere, where ozone photochemistry is faster. Of course, the relaxation times in Fig. 1 show a similar picture, but we are now able to compare between all the terms in the parametrization.

EGU

Figure 3a shows that the $(P-L)_0$ term is in general small compared to the response of the other terms to representative perturbations, and its magnitude is generally similar in all schemes. The major exception is LINOZ, where above 10 hPa the $(P-L)_0$ term is much larger than in the other schemes. Here, this term causes a strong net loss of ozone, so LINOZ generates large negative biases above 10 hPa (McCormack et al., 2004; Geer et al., 2006a). Another exception is that the $(P-L)_0$ terms in both Cariolle v1.0 and v2.1 are excessively large in the lower troposphere, being of order 10% day^{-1}. Later we see that this results in relatively large ozone biases in the lower troposphere.

Figure 3b shows that Cariolle v2.1 has relatively low sensitivity to typical ozone variability in the upper stratosphere and mesosphere, compared to the other schemes. Equivalently, this means that photochemical relaxation times are substantially longer in Cariolle v2.1.

Both the Cariolle v1.0 and v2.1 schemes are up to a factor of 10 more sensitive than LINOZ and Chem2D-OPP to ozone variations in the lower stratosphere and at the tropopause. In terms of photochemical relaxation time, this corresponds to $\tau \sim 100$ days (Fig. 1) at the tropopause compared to τ approaching 1000 days in LINOZ and Chem2D. This difference was noted by McCormack et al. (2004), though it is now thought that the rapid changes in ozone they found in Cariolle v1.0 hindcast experiments at high northern latitudes in the mid-stratosphere (around 10 hPa, their Fig. 11), which were attributed to the shorter relaxation time, were in fact most likely due to the very strong radiation term in Cariolle v1.0.

Recently updated calculations of the Chem2D-OPP coefficients (not examined here) include catalytic cycles involving bromine compounds (Br$_x$), producing somewhat shorter values of τ in the lower stratosphere, but these values remain longer than corresponding ones in the Cariolle v1.0 scheme. It must be noted that the Cariolle schemes and Chem2D-OPP use different methods to compute the relaxation time. In Cariolle's schemes it is computed after allowing for readjustment of the concentrations of short lived species in response to the ozone perturbation, whereas Chem2D-OPP

takes an instantaneous value. In the middle and upper stratosphere where the ozone production is dominated by the photodissociation of O_2 the two methods should converge. However, the two approaches may differ in the lower stratosphere where, for example, readjustments in the amount of NO_x species will have a significant effect on ozone production. The validity of each approach would depend on the timescales of the perturbations: for fast perturbations the instantaneous approach should be valid; for perturbations with timescales longer than a day, the readjustment of minor species should be taken into account.

Figure 3c shows that Chem2D-OPP v2.1 has a stronger response to temperature perturbations than does Cariolle v2.1 in the upper stratosphere and mesosphere. Cariolle v1.0 and LINOZ are a little more sensitive still. We later see that the discrepancy between the analysed and climatological temperatures (Fig. 2) is the partial cause of problems in our experiments in the upper stratosphere. The discrepancies have a larger effect in the Chem2D-OPP v2.1 experiment than in Cariolle v2.1, partly because of this stronger sensitivity to temperature.

Figure 3d shows that the Cariolle v1.0 radiation term is excessively strong compared to other schemes. In these, the influence of the radiation term is typically smaller than that of the ozone or temperature terms. It is not clear why the Cariolle v1.0 term should be so strong, since similar methods were used to create v1.0 and v2.1. Since the v1.0 coefficients were distributed many years ago it is not now possible to re-examine this in detail. The strong Cariolle v1.0 radiation term was responsible for the problem of excessive creation of ozone in the ozone hole described in Geer et al. (2006b) and the rapid ozone changes see in hindcast experiments at 10 hPa by McCormack et al. (2004, their Fig. 11).

EGU

3 Method

3.1 Assimilation system

The Met Office NWP system has recently been extended to allow the assimilation of ozone (Jackson and Saunders, 2002; Jackson, 2004) but ozone is not assimilated operationally. Here, MIPAS v4.61 ozone is assimilated in re-analysis mode, alongside all operational dynamical observations, using a stratosphere/troposphere version of the operational NWP system. The system is that described in Geer et al. (2006a), except that MIPAS temperatures are no longer assimilated, since it was found that their assimilation could degrade analysed stratopause temperatures. The GCM has a horizontal resolution of 3.75° longitude by 2.5° latitude and 50 levels in the vertical, from the surface to ~0.1 hPa. It uses a new dynamical core (Davies et al., 2005) which includes a semi-Lagrangian transport scheme. The ozone tracer is subject to convective and boundary layer transport. There is no feedback between ozone and radiation: heating rate calculations are done using an ozone climatology. Data assimilation uses 3D-Var (Lorenc et al., 2000). Ozone is assimilated univariately, but 3D-Var does not infer dynamical information, so the only effect of ozone on the dynamical analysis is through its influence on temperature radiance assimilation.

3.2 Experiments

Table 2 summarises the ozone chemistry characteristics of the six assimilation experiments performed here, which were otherwise identical. Experiments were initialised on 23 September 2003 with fields from the DARC/Met Office analyses produced for the ASSET intercomparison and described in Geer et al. (2006a). The experiments were run until 5 November 2003, capturing the period of the deepest extent of the ozone hole, as well as much synoptic variability linked with the breakdown of the SH polar vortex (Lahoz et al., 2006) and the development of the NH polar vortex.

Title Page

Abstract	Introduction
Conclusions	References
Tables	Figures

| ◄◄ | ►► |
| ◄ | ► |

| Back | Close |

Full Screen / Esc

Printer-friendly Version

Interactive Discussion

[EGU](#)

3.3 Validation framework

Analyses are compared to independent data from ozonesonde and HALOE, and to the assimilated MIPAS observations, using the methods described in Geer et al. (2006a). Analyses are interpolated onto a set of fixed pressure levels and sampled daily at 00:00 Z and 12:00 Z, before being compared to observations. The observations are described briefly below; see Geer et al. (2006a) for further details. It is worth noting that MIPAS, sonde and HALOE have different temporal and spatial sampling. For example MIPAS sampled most latitudes daily; HALOE observations come from discrete latitude bands (see coverage plots in Geer et al., 2006a). Hence, some differences are to be expected when comparing to different datatypes, simply because of the varying geographical and temporal coverage.

3.3.1 MIPAS

The only assimilated ozone observations come from MIPAS, which is an interferometer for measuring infrared emissions from the atmospheric limb (Fischer and Oelhaf, 1996). MIPAS operational data are available between July 2002 and March 2004, after which instrument problems meant it could only be used on an occasional basis. The operational measurements were made along 17 discrete lines-of-sight in the reverse of the flight direction of ENVISAT, with tangent heights between 8 km and 68 km. The vertical resolution was ∼3 km in the stratosphere and the horizontal resolution was ∼300 km along the line of sight. ENVISAT follows a sun-synchronous polar orbit, allowing MIPAS to sample globally, and to produce up to ∼1000 atmospheric profiles per day. From the infrared spectra, ESA retrieved profiles of pressure, temperature, ozone, water vapour, HNO_3, NO_2, CH_4 and N_2O at up to 17 tangent points (ESA, 2004). MIPAS version 4.61 data, reprocessed offline, is used here. When treated as a point retrieval, MIPAS ozone has only small biases when compared to independent data except in the lower stratosphere (100 to 30 hPa), where positive biases of order 10% are seen (Geer et al., 2006a).

3.3.2 Ozonesondes

Ozonesondes are used as independent data to validate the analyses. Profiles have been obtained from the World Ozone and Ultraviolet Radiation Data Centre (WOUDC, http://www.woudc.org/), Southern Hemisphere Additional Ozonesondes project (SHADOZ, http://croc.gsfc.nasa.gov/shadoz/, Thompson et al., 2003a,b) and the Network for the Detection of Stratospheric Change (NDSC, http://www.ndsc.ncep. noaa.gov/). We use ozonesonde ascents from 42 locations. Sondes typically make measurements from the surface to around the 10 hPa level. Total error for the most common type of ozonesonde is estimated to be within −7% to +17% in the upper troposphere, ±5% in the lower stratosphere up to 10 hPa and −14% to +6% at 4 hPa (Komhyr et al., 1995). Errors are higher in the presence of steep ozone gradients and where ozone amounts are low.

3.3.3 HALOE

HALOE (Russell et al., 1993) is used as independent data to validate the analyses. HALOE uses solar occultation to derive atmospheric constituent profiles, making the data sparse in time and space, with about 15 observations per day at each of two latitudes. The horizontal resolution is 495 km along the orbital track and the vertical resolution is about 2.5 km. We use a version 19 product, screened for cloud using the algorithm of Hervig and McHugh (1999), and available from the HALOE website (http://haloedata.larc.nasa.gov/). Version 19 ozone retrievals are nearly identical to those of v18, and above the 120 hPa level they agree with ozonesonde data to within 10% (Bhatt et al., 1999). Below this level, profiles can be seriously affected by the presence of aerosols and cirrus clouds.

EGU

4 Results

Figures 5, 6 and 7 show, respectively, the mean differences between analyses and HALOE, sonde and MIPAS observations, given as a percentage relative to an ozone climatology. This ozone climatology is described in Geer et al. (2006a) and combines those of Fortuin and Kelder (1998) and Logan (1999). Statistics are calculated for the period 27 September 2003 to 5 November 2003.

In the troposphere, upper stratosphere and mesosphere, and polar vortex, there are differences between experiments. Here, biases between analyses and independent data can in general be attributed to the ozone photochemistry schemes. In the lower stratosphere (100 to 10 hPa), away from the ozone hole, biases are unconnected with the photochemistry schemes. Geer et al. (2006a) show that positive biases of up to 20% against sonde and HALOE are likely explained both by the small (∼10%) positive bias in MIPAS in these regions, and by poor quality transport, a known deficiency in stratospheric data assimilation systems. These biases are a particular problem at the tropical tropopause, where the DARC/Met Office analyses are 50% higher than ozonesondes. Similar biases were found in many ozone analysis systems, though the DARC/Met Office analyses have an atypically large bias at the tropopause.

We also examined the standard deviations of difference between analyses and observations. The results were in general very similar to those seen in Geer et al. (2006a), and typical of many ozone data assimilation systems. Significant differences between experiments were found only in the SH high latitude upper stratosphere, shown in Fig. 8.

The following sections examine these biases and standard deviations at different levels in the atmosphere.

4.1 Upper stratosphere and mesosphere

In the upper stratosphere and mesosphere, the LINOZ scheme produces negative ozone biases that reach 40 to 50% at 0.5 hPa (Figs. 5 and 7). This is a known problem

with the scheme (McCormack et al., 2004; Geer et al., 2006a).

There are positive biases in Chem2D-OPP v2.1 analyses in the upper stratosphere (1 hPa to 10 hPa), reaching 20% in SH high latitudes, compared both to MIPAS and HALOE. In the same region, Chem2D-OPP v2.1 shows the largest standard deviations against MIPAS and HALOE of any of the analyses, reaching 20% against MIPAS (Fig. 8), though in other latitude bands (not shown) there is little difference between experiments. Figure 9 shows examples of the analysed ozone fields at 3.2 hPa. It appears that, at latitudes 60°S to 90°S, Cariolle v2.1 represents the observed ozone field quite realistically, with standard deviations of ~6% against HALOE and MIPAS (Fig. 8). In contrast, Cariolle v1.0 and Chem2D-OPP v0.1 have standard deviations of ~10%, suggesting that the smaller range of ozone values in these analyses over the poles (Fig. 9) is less in agreement with independent data. Structure seen in the ozone field over the pole in the Chem2D v2.1 analyses is likely erroneous, given the much larger (~20%) standard deviations.

The most likely explanation for the erroneous structure in the Chem2D-OPP v2.1 ozone fields is in the temperature term. We have already seen that the CIRA86 temperature climatology used with Chem2D is substantially different from the modelled temperatures (Fig. 2). Chem2D-OPP v0.1, without a temperature term, performs better in this region. During the vortex breakup, temperature structures are often far from zonal mean, as can be seen from Fig. 10. Examination of the individual terms shows that the strongly non-zonal temperature field causes the temperature term in Eq. (1) to drive ozone amounts away from the zonal mean. In opposition, it is mainly the ozone term that returns ozone amounts to zonal mean. The influence of the radiation and $(P-L)_0$ terms is relatively weak. The Chem2D-OPP v2.1 temperature term rate coefficient is substantially more sensitive than that in the Cariolle v2.1 scheme (Fig. 3), enhancing the effect of the biased temperature climatology.

Cariolle v2.1 shows positive biases (Figs. 5 and 7) at 1 hPa and above, reaching a maximum of 20% in the tropics at 0.5 hPa. Biases against both HALOE and MIPAS are typically smaller, though not eliminated, when the Fortuin and Kelder (1998) clima-

EGU

tology is used instead of the supplied climatology. This suggests that the climatology supplied with the Cariolle v2.1 scheme is slightly biased at these levels, and that replacing it with the Fortuin and Kelder (1998) climatology can remove part of this bias. However, even after doing this, there are still biases of order 10% in the analyses versus HALOE. Following the arguments in Sect. 2.1.1, it is likely the biases could be further reduced by fine-tuning the temperature climatology (T_0) and making the ozone climatology (χ_0) consistent with climatological ozone amounts from MIPAS. However, MIPAS and HALOE are biased by ∼5% with respect to each other at these levels (Geer et al., 2006a), so even if the model was consistent with MIPAS, there would necessarily be a bias compared to HALOE. Moreover, this would improve the simulation for the period studied without guarantee of its applicability for other seasons.

In summary, in the upper stratosphere and mesosphere, LINOZ is unsuitable for use, and there are regional biases in the Cariolle v2.1 and Chem2D-OPP v2.1 experiments (respectively, the tropical mesosphere and the upper stratospheric winter vortex). With further attention to the temperature and ozone climatologies, T_0 and χ_0, these latter biases would likely be reduced. Excluding LINOZ, and Cariolle v2.1 and Chem2D v2.1 in the problem regions, analyses show biases in the range –10% to 10%.

4.2 Lower stratosphere

At SH high latitudes at the levels where ozone depletion takes place in the ozone hole (100 to 40 hPa), the Cariolle v1.0 experiment shows roughly 20% too much ozone compared to HALOE and sonde. As explained in more detail in Geer et al. (2006b), the strong radiation term of the v1.0 parametrization (Fig. 3d) creates erroneously large amounts of ozone in the ozone hole. The other experiments show positive biases of no more than 10%, confirming that they work well in conjunction with the cold tracer heterogeneous chemistry scheme. The biases against MIPAS are smaller still, indicating that the analyses have drawn close to the assimilated MIPAS observations and the remaining biases against independent data reflect the ∼10% positive bias between MIPAS and independent data in these regions (Geer et al., 2006a).

At the tropical and midlatitude tropopause, comparisons against independent data show no difference between experiments. This is despite an order of magnitude difference in the sensitivity of the ozone terms in Cariolle v2.1 and Chem2D-OPP (Fig. 3b). Photochemical relaxation times are in both cases extremely long ($\sim$100 days and $\sim$1000 days, respectively), meaning that the chemistry schemes are a minor part of the ozone budget here, which is dominated by transport and observational increments. Hence, evaluation within a data assimilation system is not able to distinguish between the parametrizations or to suggest which may be more correct. Differences would only appear in relatively long free-model runs, which would also require a very good representation of tracer transport.

4.3 Troposphere

In the troposphere, there are biases of -50% to $+100\%$ against sonde (Fig. 6). No ozone observations are assimilated below approximately 400 hPa; the assimilation system must rely on modelled ozone photochemistry and transport.

The largest biases tend to be associated with the Cariolle scheme: Cariolle v1.0 has a positive bias of over 100% in the SH polar troposphere, while Cariolle v2.1 has a positive bias of 80% in the tropical lower troposphere. The latter bias has also been seen in assimilation runs with the MOCAGE/PALM data assimilation system using Cariolle v2.1 photochemistry (Geer et al., 2006a). By a detailed examination of the coefficients (not shown), it appears that these positive biases arise because of ozone production by the $(P-L)_0$ term, which is substantially larger than those in LINOZ or Chem2D-OPP in the lower troposphere. Figure 3a gives some indication of this. This model bias in the equatorial lower troposphere has been mostly corrected in v2.3 of the Cariolle scheme (Cariolle and Teyssédre, 2006[1]), but has not been tested in this study since we focus on the results of assimilation experiments that use data present only above $\sim$400 hPa.

Other schemes are, because of the way they have been implemented in these experiments, dominated by the relaxation to climatology of the ozone term. For these schemes, biases are in general within -20% to $+20\%$, except in the NH polar lower

Title Page

Abstract | Introduction

Conclusions | References

Tables | Figures

◄◄ | ►►

◄ | ►

Back | Close

Full Screen / Esc

Printer-friendly Version

Interactive Discussion

EGU

troposphere, where biases can be as large as −40%, though results are based on very few sondes. The correct handling of tropospheric ozone remains an outstanding challenge in ozone data assimilation. Hence, a pragmatic temporary solution is to relax ozone amounts to climatology. In these experiments it is a 2-D climatology, but use of a 3-D one like Logan (1999) would capture the main zonal features of the tropospheric ozone distribution, which are visible in total column observations in the tropics. This would be important if total column observations were assimilated, so as to avoid the aliasing of tropospheric biases into changes in stratospheric ozone.

5 Conclusion

This study has examined ozone analyses from the Met Office stratosphere/troposphere data assimilation system. MIPAS ozone retrievals were assimilated for the period 23 September 2003 until 5 November 2003 into a set of experiments, each using a different linear ozone photochemistry parametrization. Heterogeneous chemistry was parametrized using a cold tracer scheme (Eskes et al., 2003), and remained fixed throughout the experiments. Analysed ozone was validated against independent observations from HALOE and ozonesondes. None of the ozone parametrizations is specifically intended for use in the troposphere, where modelling and observing ozone remains a substantial challenge, but results were in general good in the stratosphere and mesosphere.

In the mid and lower stratosphere, analyses strongly benefitted from the assimilation of good quality MIPAS data with a relatively high vertical resolution. A system with more sparse observational coverage for ozone (typical of operational systems) would reveal larger biases and differences between the photochemistry schemes. However, in the upper stratosphere and mesosphere, the photochemical lifetime of ozone is short, and analyses at these levels are controlled mostly by the ozone parametrization, not by the assimilated observations.

In summary, we found:

EGU

- LINOZ is unsuitable for use above 10 hPa (McCormack et al., 2004; Geer et al., 2006a), though below this level, it generally works as well as the other schemes.

- Cariolle v1.0 has an excessively strong dependence on overlying column ozone in the radiation term (Geer et al., 2006b), which causes excessive ozone production in the ozone hole, leading to ozone values 20% higher than sonde in the SH lower stratosphere (100 to 30 hPa) in the current experiments. There are also unrealistically high ozone values near the surface around Antarctica. Since these coefficients were generated many years ago (Cariolle and Déqué, 1986), it is hard to identify exactly where these problems may have come from. Elsewhere, Cariolle v1.0 works in general as well as the other schemes.

- The Cariolle v2.1 scheme performed well in general. A $\sim$20% positive bias in the tropical upper stratosphere and mesosphere was caused largely by the supplied ozone climatology, and could be partially corrected by substituting the Fortuin and Kelder (1998) climatology. There was also an 80% positive bias in the tropical lower troposphere, linked to excessive ozone production in the $(P-L)_0$ term, which has been largely corrected in a new version of the scheme (v2.3, not tested here). Cariolle v2.1 analyses had particular success in the SH high latitude upper stratosphere (6 hPa to 1 hPa), which experienced strong minor warmings through October 2003, with synoptic temperature variations of $\sim$50 K. Here, Cariolle v2.1 analyses showed only 6% standard deviation of difference against HALOE, compared to 10% for most other schemes and 20% for Chem2D-OPP v2.1.

- Analyses using Chem2D-OPP v0.1 (only the first two terms in Eq. 1) and v2.1 (all terms) performed well in general. Chem2D-OPP v2.1 produced unrealistic ozone structures in the SH polar upper stratosphere (6 hPa to 1 hPa), likely due to discrepancies between analysed temperatures and the CIRA86 temperature climatology supplied with the scheme. The problem is likely to have been exacerbated by a larger sensitivity to temperature variations than is found in the

Cariolle v2.1 scheme. A new temperature climatology is currently being tested with a new version of the Chem2D-OPP scheme, and shows promising results.

These tests are based on a short period in September to November. The precise behaviour, for example in terms of the bias in any scheme, is likely to vary from region to region and through the year. Nevertheless, many of the problems we have illustrated are explained by specific features of the coefficients in the various schemes. These features are persistent throughout the year, and can be seen in versions of Fig. 3 for other months (not shown). Hence, similar problems can be expected in other months.

This paper illustrates the problems that can be caused when there are discrepancies between the climatologies of temperature and ozone used within the ozone parametrization and their equivalents in the GCM and in the assimilated observations. Improvements could be made by making the climatologies of ozone and temperature in the schemes more consistent with their equivalents in the GCM. In data assimilation applications, models should also be unbiased with respect to observations. In regions where the photochemical lifetime is short, this means the schemes should if possible use an ozone climatology based on the assimilated data.

Future developments of the ozone photochemistry schemes could include a better treatment of the troposphere. Also, none of these schemes simulates the diurnal cycle of ozone above 0.5 hPa, yet this has a strong influence modelled temperatures (Sassi et al., 2005).

We have noted that these analyses strongly benefit from the assimilation of good quality MIPAS data, and that in other circumstances, differences between the photochemical schemes would be more obvious. A particular example is the differing relaxation times (τ) in the Cariolle and Chem2D-OPP schemes in the lower stratosphere. The schemes use different methods to calculate τ, resulting in an order of magnitude difference in the sensitivity to ozone variations in the lower stratosphere (100 to 30 hPa, Fig. 3 and McCormack et al., 2004). Despite this, we see no difference between experiments. Photochemical timescales are relatively slow here (>100 days); any slow-growing model biases would be corrected by the observation increments, which are

Linear ozone photochemistry parametrizations

A. J. Geer et al.

Title Page

Abstract	Introduction
Conclusions	References
Tables	Figures

◄◄   ►►

◄   ►

Back   Close

Full Screen / Esc

Printer-friendly Version

Interactive Discussion

EGU

added on much shorter timescales. Hence, data assimilation is best for testing the photochemistry schemes in regions where they have a more dominant control on the ozone amounts, such as in the mid and upper-stratosphere. Data assimilation does however force the schemes to operate in an environment as close to reality as can be provided, which model free-runs cannot do. However, it is clear that the results in this paper would be usefully complemented by long-term GCM or CTM runs which would allow slow-growing problems to be identified, and by comparisons to more detailed chemistry schemes.

References

Bhatt, P. P., Remsberg, E. E., Gordley, L. L., McInerney, J. M., Brackett, V. G., and Russell, J. M.: An evaluation of the quality of Halogen Occultation Experiment ozone profiles in the lower stratosphere, J. Geophys. Res., 104, 9261–9275, 1999. 7445

Cariolle, D. and Déqué, M.: Southern-Hemisphere Medium-Scale Waves and Total Ozone Disturbances in a Spectral General Circulation Model, J. Geophys. Res., 91, 10 825–10 846, 1986. 7429, 7430, 7436, 7451, 7458

Cariolle, D. and Morcrette, J.-J.: A linearized approach to the radiative budget of the stratosphere: influence of the ozone distribution, Geophys. Res. Lett., 33, L05806, doi:10.1029/2005GL025597, 2006. 7430

ACPD

6, 7427–7469, 2006

Linear ozone photochemistry parametrizations

A. J. Geer et al.

Title Page

Abstract | Introduction

Conclusions | References

Tables | Figures

◄ | ►

◄ | ►

Back | Close

Full Screen / Esc

Printer-friendly Version

Interactive Discussion

EGU

Chipperfield, M. P.: Multiannual simulations with a three-dimensional chemical transport model, J. Geophys. Res., 104, 1781–1805, 1999. 7429

Davies, T., Cullen, M. J. P., Malcolm, A. J., Mawson, M. H., Staniforth, A., White, A. A., and Wood, N.: A new dynamical core for the Met Office's global and regional modelling of the atmosphere, Quart. J. Roy. Meteorol. Soc., 131, 1759–1782, 2005. 7443

Dethof, A. and Hólm, E. V.: Ozone assimilation in the ERA-40 reanalysis project, Quart. J. Roy. Meteorol. Soc., 130, 2851–2872, 2004. 7429, 7458

DeMore, W. B., Sander, S. P., Golden, D. M, Hampson, R. F., Kurylo, M. J., Howard, C. J., Ravishankara, A. R., Kolb, C. E., and Molina, M. J.: Chemical kinetics and photochemical data for use in stratospheric modelling, in Evaluation 12, JPL Publ. 97-4, Jet Propul. Lab, Pasadena, Calif., available from http://jpldataeval.jpl.nasa.gov/, 1997. 7438

Errera, Q. and Fonteyn, D.: Four-dimensional chemical data assimilation of CRISTA stratospheric measurements, J. Geophys. Res., 106, 12 253–12 265, 2001. 7429

European Space Agency: MIPAS Product Handbook, issue 1.2, available from http://envisat.esa.int/dataproducts, 2004. 7444

Eskes, H. J., Van Velthoven, P. F. J., Valks, P. J. M., and Kelder, H. M.: Assimilation of GOME total-ozone satellite observations in a three-dimensional tracer-transport model, Quart. J. Roy. Meteorol. Soc., 129, 1663–1681, 2003. 7429, 7434, 7436, 7437, 7450

Eskes, H. J., Segers, A. J., and Van Velthoven, P. F. J.: Ozone forecasts of the Stratospheric Polar Vortex Splitting Event in September 2002, J. Atmos. Sci., 62, 812–821, 2005. 7436

Fischer, H. and Oelhaf, H.: Remote sensing of vertical profiles of atmospheric trace constituents with MIPAS limb-emission spectrometers, Appl. Opt., 35, 2787–2796, 1996. 7444

Fortuin, J. P. F. and Kelder, H.: An ozone climatology based on ozonesonde and satellite measurements, J. Geophys. Res., 103, 31 709–31 734, 1998. 7435, 7437, 7438, 7440, 7446, 7447, 7448, 7451, 7459

Geer, A. J., Lahoz, W. A., Bekki, S., Bormann, N., Errera, Q., Eskes, H. J., Fonteyn, D., Jackson, D. R., Juckes, M. N., Massart, S., Peuch, V.-H., Rharmili, S., and Segers, A.: The ASSET intercomparison of ozone analyses: method and first results, Atmos. Chem. Phys. Discuss., 6, 4495–4577, 2006a. 7429, 7430, 7432, 7436, 7437, 7438, 7441, 7443, 7444, 7446, 7447, 7448, 7449, 7451

Geer, A. J., Peubey, C., Bannister, R. N., Brugge, R., Jackson, D. R., Lahoz, W. A., Migliorini, S., O'Neill, A., and Swinbank, R.: Assimilation of stratospheric ozone from MIPAS into a global general circulation model: the September 2002 vortex split, Quart. J. Roy. Meteorol.

Title Page

Abstract | Introduction

Conclusions | References

Tables | Figures

◄◄ | ►►

◄ | ►

Back | Close

Full Screen / Esc

Printer-friendly Version

Interactive Discussion

EGU

Soc., 132, 231–257, 2006b. 7429, 7430, 7434, 7442, 7448, 7451

Hadjinicolaou, P., Pyle, J. A., Chipperfield, M. P., and Kettleborough, J. A.: Effect of interannual meteorological variability on mid-latitude O_3, Geophys. Res. Lett., 24, 2993–2996, 1997. 7429

5 Hervig, M. and McHugh, M.: Cirrus detection using HALOE measurements, Geophys. Res. Lett., 26, 719–722, 1999. 7445

Jackson, D. R.: Improvements in data assimilation at the Met Office, Met Office Forecasting Research Technical Report, 454, available from Met Office, UK, 2004. 7443

Jackson, D. R. and Saunders, R.: Ozone Data Assimilation: Preliminary System, Met Office
10 Forecasting Research Technical Report, 394, available from Met Office, UK, 2002. 7443

Josse, B., Simon, P., and Peuch, V.-H.: Radon global simulations with the multiscale chemistry and transport model MOCAGE, Tellus, 56B, 339–356, 2004. 7429

Jet Propulsion Laboratory: Chemical Kinetics and Photochemical Data for Use in Atmospheric Studies: Evaluation Number 14, JPL publication 02-25, Jet Propulsion Laboratory, California
15 Institute of Technology, Pasadena, California, USA, available from http://jpldataeval.jpl.nasa. gov/, 334 pp., 2003. 7437, 7438

Komhyr, W. D., Barnes, R. A., Brothers, G. B., Lathrop, J. A., and Opperman, D. P.: Electrochemical Concentration Cell Ozonesonde Performance Evaluation During STOIC 1989, J. Geophys. Res., 100, 9231–9244, 1995. 7445

20 Lahoz, W. A., Geer, A. J., and O'Neill, A.: Dynamical evolution of the 2003 Southern Hemisphere stratospheric winter using Envisat trace-gas observations, Quart. J. Roy. Meteorol. Soc., accepted, 2006. 7435, 7443

Logan, J. A.: An analysis of ozonesonde data for the troposphere: Recommendations for testing 3-D models and development of a gridded climatology for tropospheric ozone, J.
25 Geophys. Res., 104, 16 115–16 149, 1999. 7446, 7450

Lorenc, A. C., Ballard, S. P., Bell, R. S., Ingleby, N. B., Andrews, P. L. F., Barker, D. M., Bray, J. R., Clayton., A. M., Dalby, T. D., Li, D., Payne, T. J., and Saunders, F. W.: The Met. Office global three-dimensional variational data assimilation scheme, Quart. J. Roy. Meteorol. Soc., 126, 2991–3012, 2000. 7443

30 McCormack, J. P., Eckermann, S. D., Coy, L., Allen, D. R., Kim, Y.-J., Hogan, T., Lawrence, B., Stephens, A., Browell, E. V., Burris, J., McGee, T., and Trepte, C. R.: NOGAPS-ALPHA model simulations of stratospheric ozone during the SOLVE2 campaign, Atmos. Chem. Phys., 4, 2401–2423, 2004. 7429, 7430, 7438, 7439, 7441, 7442, 7447, 7451, 7452,

Linear ozone photochemistry parametrizations

A. J. Geer et al.

Title Page

Abstract	Introduction
Conclusions	References
Tables	Figures

◄ | ►|

◄ | ►

Back | Close

Full Screen / Esc

Printer-friendly Version

Interactive Discussion

EGU

7458

McCormack, J. P., Eckermann, S. D., Siskind D. E., and Coy, L.: A new linearized gas-phase ozone photochemistry parameterization for high-altitude NWP and climate models, Atmos. Chem. Phys. Discuss., 6, 6627–6694, 2006. 7438, 7439, 7458

McLinden, C. A., Olsen, S. C., Hannegan, B., Wild, O., Prather, M. J., and Sundet, J.: Stratospheric ozone in 3-D models: A simple chemistry and the cross-tropopause flux, J. Geophys. Res., 105, 14 653–14 665, 2000. 7429, 7433, 7437, 7458

McPeters, R.: Ozone profile comparisons, in: The Atmospheric Effects of Stratospheric Aircraft: Report of the 1992 Models and Measurements Workshop, NASA Ref. Publ. 1292, edited by: Prather, M. J. and Remsberg, E. E., D1–D37, 1993. 7438

Nagatani, R. M. and Rosenfield, J. E.: Temperature, net heating and circulation, in: The Atmospheric Effects of Stratospheric Aircraft: Report of the 1992 Models and Measurements Workshop, NASA Ref. Publ. 1292 edited by: Prather, M. J. and Remsberg, E. E., A1–A47, 1993. 7438

Plumb, R. A.: Stratospheric transport, J. Meteorol. Soc. Jpn., 80, 793–809, 2002. 7433

Prather, M. J.: Catastrophic loss of stratospheric ozone in dense volcanic clouds, J. Geophys. Res., 97, 10 187–10 191, 1992. 7437

Prather, M. J. and Jaffe, A. H.: Global impact of the antarctic ozone hole: Chemical propagation, J. Geophys. Res., 95, 3473–3492, 1990. 7437

Randel, W., Udelhofen, P., Fleming, E., Geller, M., Gelman, M., Hamilton, K., Karoly, D., Ortland, D., Pawson, S., Swinbank, R., Wu, F., Baldwin, M., Chanin, M. L., Keckhut, P., Labitzke, K., Remsberg, E., Simmons, A., and Wu, D.: The SPARC intercomparison of middle-atmosphere climatologies, J. Climate, 17, 986–1003, 2004. 7435

Rozanov, E. V., Zubov, V. A., Schlesinger, M. E., Yang, F., and Andronova, N. G.: The UIUC three-dimensional stratospheric chemical transport model: Description and evaluation of the simulated source gases and ozone, J. Geophys. Res., 104, 11 755–11 781, 1999. 7429

Russell, J. M., Gordley, L. L., Park, J. H., Drayson, S. R., Hesketh, W. D., Cicerone, R. J., Tuck, A. F., Frederick, J. E., Harries, J. E., and Crutzen, P. J.: The Halogen Occultation Experiment, J. Geophys. Res., 98, 10 777–10 797, 1993. 7445

Sassi, F., Boville, B. A., Kinnison, D., and Garcia, R. R.: The effects of interactive ozone chemistry on simulations of the middle atmosphere, Geophys. Res. Lett., 32, L07811, doi:10.1029/2004GL022131, 2005. 7452

Schoeberl, M. R., Douglass, A. R., Zhu, Z. X., and Pawson, S.: A comparison of the lower

stratospheric age spectra derived from a general circulation model and two data assimilation systems, J. Geophys. Res., 108, 4113, doi:10.1029/2002JD002652, 2003. 7434

Siskind, D. E., Eckermann, S. D. , McCormack, J. P., Alexander, M. J., and Bacmeister, J. T.: Hemispheric differences in the temperature of the summertime stratosphere and meso-
5   sphere, J. Geophys. Res., 108, 4051, doi:10.1029/2002JD002095, 2003. 7438

Taylor, C. P. and Bourqui, M. S.: A new fast stratospheric ozone chemistry scheme in an intermediate general-circulation model. I: Description and evaluation, Quart. J. Roy. Meteorol. Soc., 131, 2225–2242, 2005. 7429

Thompson, A. M., Witte, J. C., McPeters, R. D., Oltmans, S. J., Schmidlin, F. J., Logan, J. A.,
10   Fujiwara, M., Kirchhoff, V. W. J. H., Posny, F., Coetzee, G. J. R., Hoegger, B., Kawakami, S., Ogawa, T., Johnson, B. J., Vomel, H., and Labow, G.: Southern Hemisphere Additional Ozonesondes (SHADOZ) 1998–2000 tropical ozone climatology – 1. Comparison with Total Ozone Mapping Spectrometer (TOMS) and ground-based measurements, J. Geophys. Res., 108, 8238, doi:10.1029/2001JD000967, 2003a. 7445

15 Thompson, A. M., Witte, J. C., Oltmans, S. J., Schmidlin, F. J., Logan, J. A., Fujiwara, M., Kirchhoff, V. W. J. H., Posny, F., Coetzee, G. J. R., Hoegger, B., Kawakami, S. J., Ogawa, T., Fortuin, J. P. F., and Kelder, H. M.: Southern Hemisphere Additional Ozonesondes (SHADOZ) 1998–2000 tropical ozone climatology – 2. Tropospheric variability and the zonal wave-one, J. Geophys. Res., 108, 8241, doi:10.1029/2002JD002241, 2003b. 7445

20 World Meteorological Organisation: Scientific assessment of ozone depletion: 2002, Global Ozone Research and Monitoring Project-Report No. 47, 498 pp., Geneva, 2003. 7429, 7436

EGU

Table 1. Linear ozone photochemistry coefficients.

Name	Notes	Reference
Cariolle v1.0		Cariolle and Déqué (1986)
Cariolle v1.2	As v1.0 but with heterogeneous chem. term	Cariolle and Déqué (1986); Dethof and Hólm (2004)
Cariolle v2.1		Cariolle and Teyssédre (2006)[1]
LINOZ		McLinden et al. (2000)
Chem2D-OPP v0.1	$(P-L)_0$ and ozone terms only	McCormack et al. (2004)
Chem2D-OPP v2.1	All four terms	McCormack et al. (2006)

Table 2. Summary of experiments.

Name	Ozone climatology, χ_0	Heterogeneous chemistry
Cariolle v1.0 with F&K climatology	Fortuin and Kelder (1998)	Cold tracer
Cariolle v2.1	Cariolle v2.1	Cold tracer
Cariolle v2.1 with F&K climatology	Fortuin and Kelder (1998)	Cold tracer
LINOZ	Fortuin and Kelder (1998)	Cold tracer
Chem2D-OPP v0.1	Fortuin and Kelder (1998)	Cold tracer
Chem2D-OPP v2.1	Fortuin and Kelder (1998)	Cold tracer

EGU
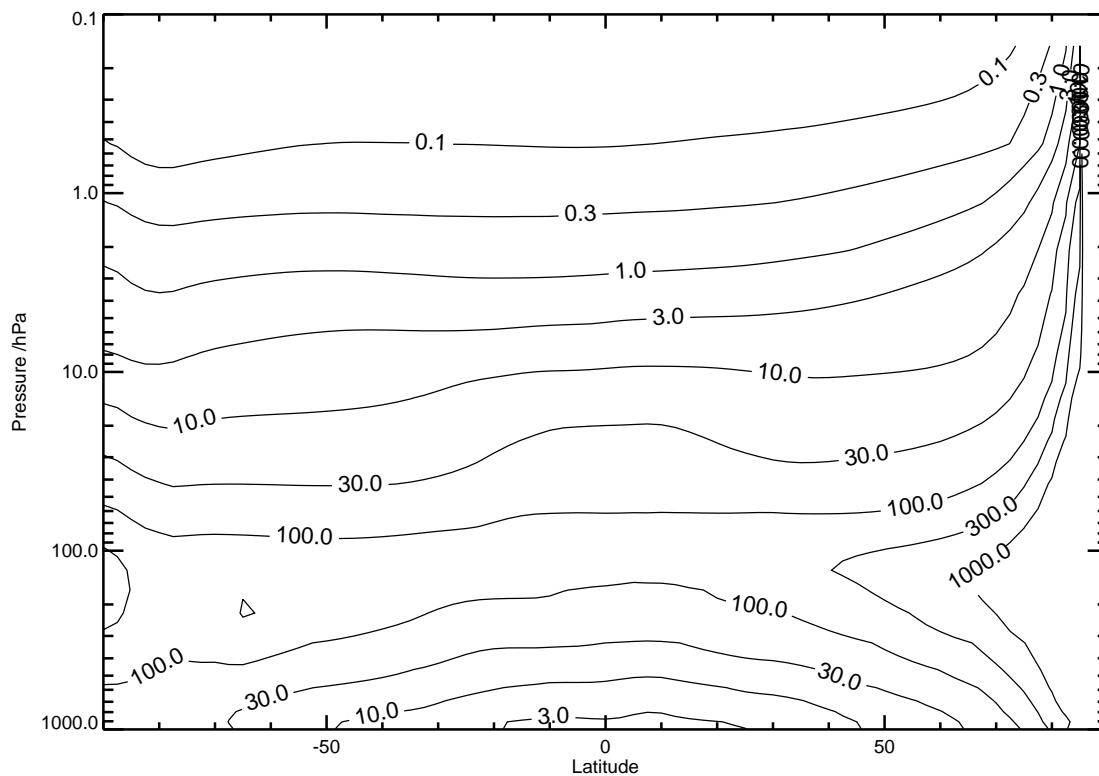
Fig. 1. October values of τ, the photochemical relaxation time, in days, from the Cariolle v1.0 parametrization.

EGU
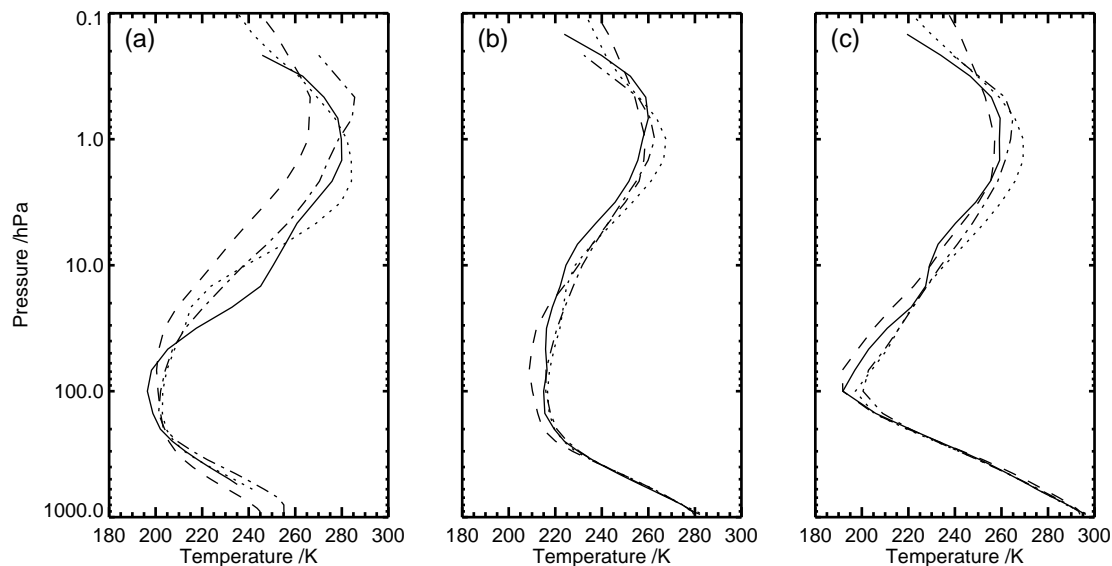
Fig. 2. October mean temperature at **(a)** 80° S, **(b)** 40° S, **(c)** the Equator, from the October 2003 DARC analyses (solid), the Cariolle v1.0 (dot-dashed) and v2.1 (dashed) coefficients, and CIRA 1986 climatology used in Chem2D OPP v2.1 (dotted).
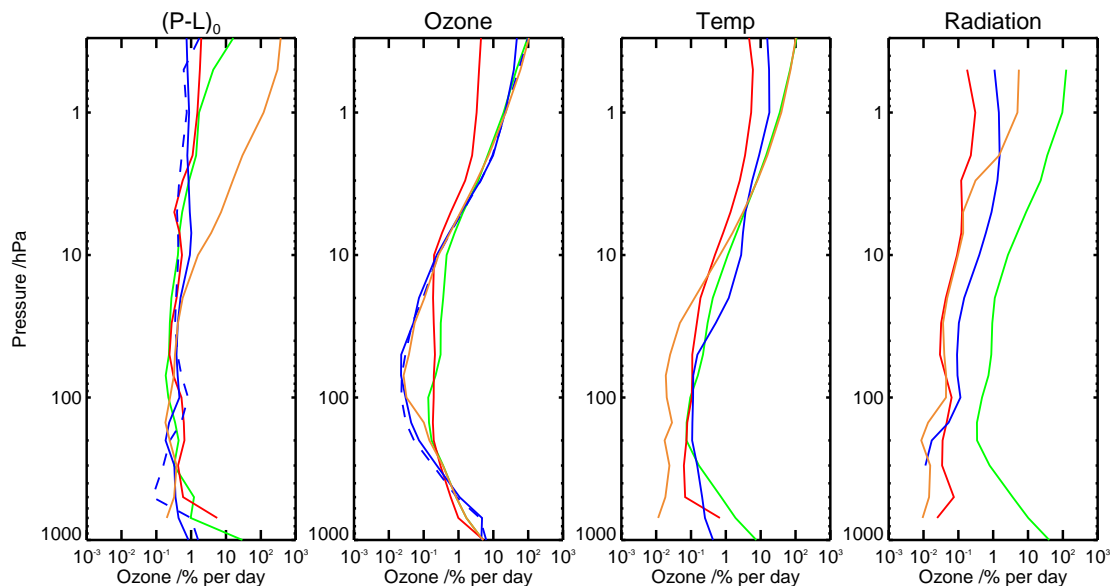
Fig. 3. Global mean absolute values of the rate of change of ozone (% per day) produced by the October coefficients of the photochemistry schemes from the $(P-L)_0$ term **(a)** and in response to typical perturbations of ozone **(b)**, temperature **(c)**, and overlying column ozone **(d)**. See colour key in Fig. 4. Note only one line is shown for Cariolle v2.1, because these values are independent of the climatology coefficients (in later figures we need to distinguish which ozone climatology was used). Also, zero rates of change cannot be shown on this figure because of the logarithmic scale; for example there is no line associated with the Chem2D-OPP v2.1 radiation term at 500 hPa and below, where this term is set to zero.

EGU

——————— Cariolle v1.0; F&K climatology

——————— LINOZ

– – – – – Chem2D OPP v0

——————— Chem2D OPP v2.1

——————— Cariolle v2.1

– – – – – Cariolle v2.1; F&K climatology

Fig. 4. Key to the analyses.
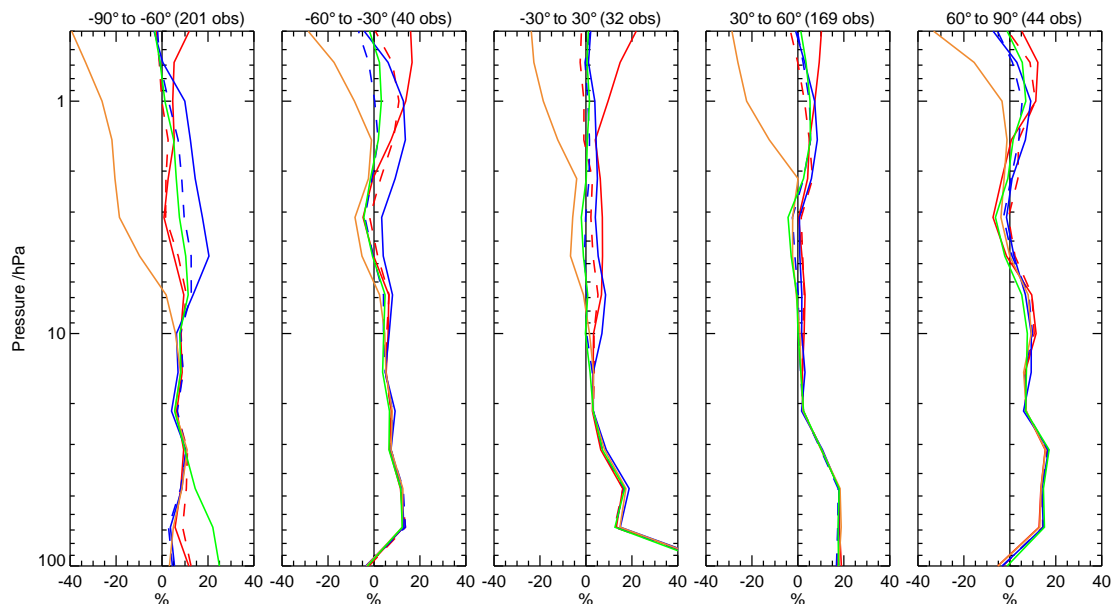
Fig. 5. Mean of (analysis – HALOE) ozone, normalised by climatology, in latitude bands for the period 27 September 2003 to 5 November 2003. See colour key in Fig. 4.

EGU
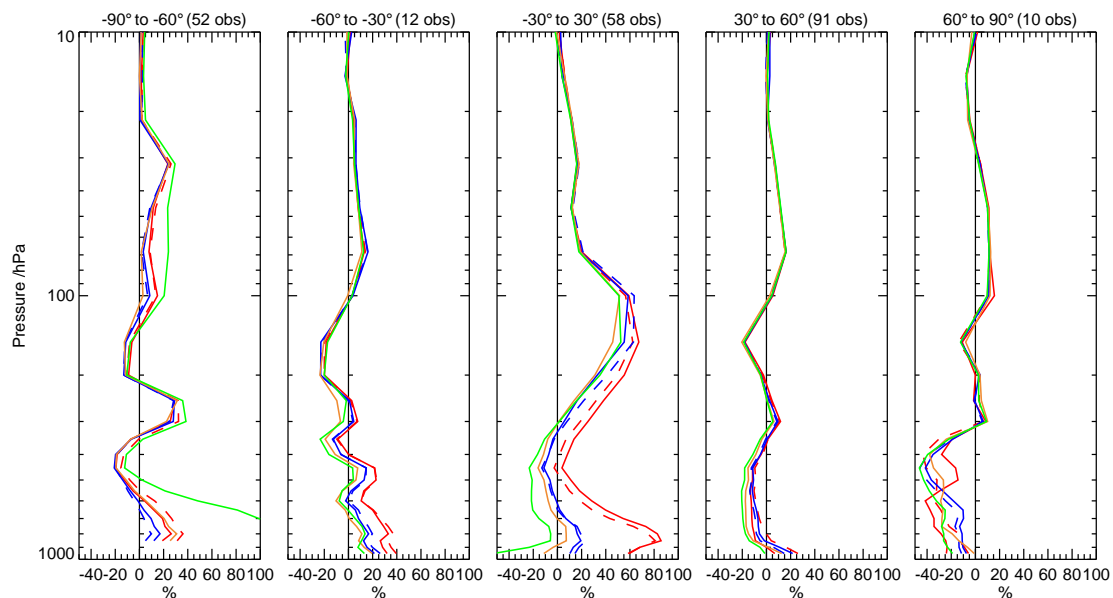
Fig. 6. Mean of (analysis – ozonesonde) ozone, normalised by climatology, in latitude bands for the period 27 September 2003 to 5 November 2003. See colour key in Fig. 4.
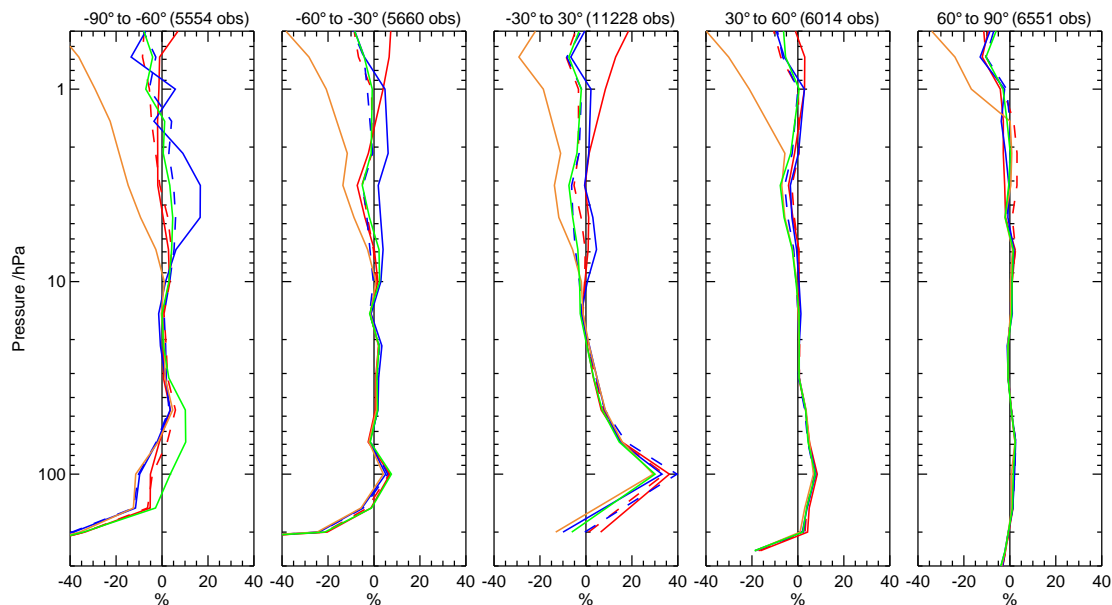
Fig. 7. Mean of (analysis – MIPAS) ozone, normalised by climatology, in latitude bands for the period 27 September 2003 to 5 November 2003. See colour key in Fig. 4.
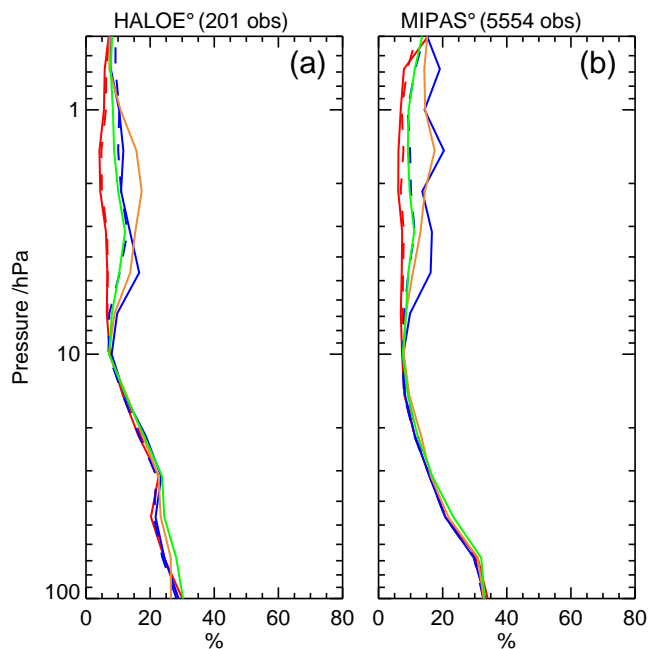
Fig. 8. Standard deviation of **(a)** (analysis – HALOE) and **(b)** (analysis – MIPAS) ozone, normalised by climatology, in the latitude band 90° S to 60° S for the period 27 September 2003 to 5 November 2003. See colour key in Fig. 4.

EGU
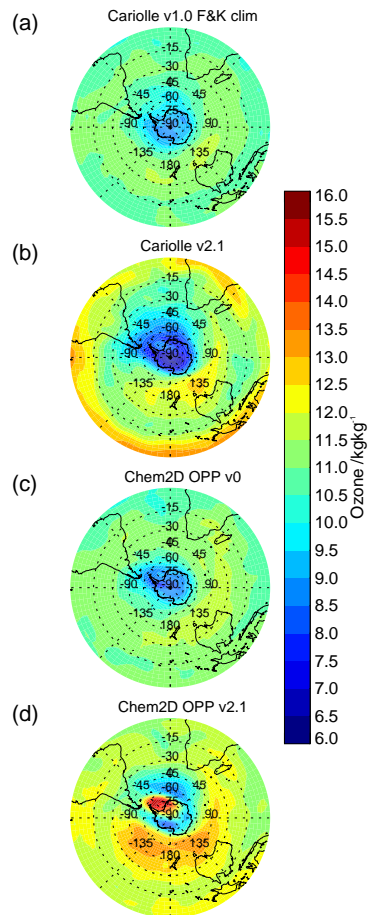
Fig. 9. Ozone fields at 3.2 hPa on 1 October 2003 from **(a)** Cariolle v1.0, **(b)** Cariolle v2.1, **(c)** Chem2D-OPP v0.1 and **(d)** Chem2D-OPP v2.1 analyses.
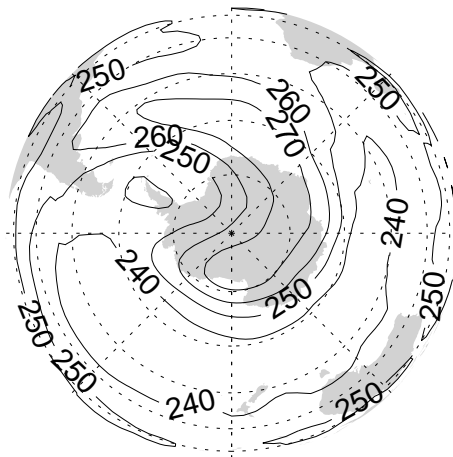
Fig. 10. Analysed temperature at 3.2 hPa on 1 October 2003.

EGU